

Breast Tissue Stiffness in Compression is Correlated to Histological Diagnosis

Parris S. Wellman

Robert D. Howe

Division of Engineering and Applied Science

Harvard University

Cambridge, MA 02143

(parris@hrl.harvard.edu, howe@deas.harvard.edu)

Edward Dalton

Northern New England Surgical Associates

Bedford, NH 03110

Kenneth A. Kern

Department of Surgery

Hartford Hospital

Hartford, CT 06115

University of Connecticut School of Medicine

Storrs, CT 06269

Abstract

Many researchers have proposed imaging the stiffness distribution in breast tissue to enhance diagnosis of disease. They suppose that cancers are much stiffer than the surrounding tissue but to our knowledge no measurements have been made of these properties that accurately characterize them over a wide range of strain. We hypothesize that there is a correlation between elastic modulus in compression and histological diagnosis (e.g. infiltrating ductal carcinoma, normal glandular tissue, etc.). We also hypothesize that the cancer exhibits greater non-linearity; its change in modulus with strain is greater. We present a correlation that allows elastic moduli to be estimated from force displacement curves measured during punch indentation testing. The tissue samples tested were obtained during surgery and were tested immediately after removal from the body. We found that there is a significant difference in the stiffness and the rate of increase in stiffness with strain between cancerous and benign breast tissues. Infiltrating ductal cancer is more than 10 times as stiff as normal fat tissue at 1% strain, and more than 70 times as stiff at 15% strain. Compared to normal glandular tissue, this type of cancer is more than 2.5 times as stiff at 1% strain and nearly 5 times as stiff at 15% strain. Therefore, relative stiffness is a good indicator of histological diagnosis.

Introduction

The contrast in elastic stiffness between normal and abnormal breast tissue has long been recognized (Harris 1994). Many researchers have proposed techniques for examining abnormal breast tissue that rely upon the elastic contrast in order to image them (Garra 1997, Lerner 1987, Chenevert 1997). Typically these techniques make images of the tissue at two different applied loads and compute a displacement field from them. This displacement field is then used to infer the stiffness of the tissue, given assumptions about the stress field. Other researchers have proposed techniques that rely on pressure distribution measurements made at the surface of the tissue when it is loaded (Gentle 1988, Sarvazyan 1997, Wellman 1999). There has even been some work to noninvasively measure the stiffness of tissue by measuring the propagation of elastic shear waves using magnetic resonance imaging (Muthupillai 1995).

While these researchers have discussed visualizing the tissue stiffness distribution within a breast, there is surprisingly little available in the literature on its mechanical properties that would allow one to draw conclusions about the histological nature of the tissue directly from the estimated stiffness. While these tissues display both a viscous (time dependent) and elastic response a large fraction of the force developed can be attributed purely to the elastic response. Given this observation, in order to develop tractable mathematical models from which to extract material properties, most researchers have idealized the tissue to be isotropic and elastic (Hayes 1971, Krouskop 1998, Sarvazyan 1995, Skovoroda 1995, Zhang 1997). In addition, the usual assumption is that the tissue is nearly incompressible (Fung 1993). With these assumptions, it is possible to model the behavior of the tissue using a single elastic or shear modulus.

Under these assumptions, Sarvazyan (1995) reported a study of 150 specimens of normal, fibroadenomatous and cancerous tissues which showed that fibroadenomas are typically 4 times as stiff as normal tissue, while cancer can be as much as 7 times as stiff. Skovoroda (1995) found that the maximum ratio was about 3:1 for cancer, and as much as 10:1 for fibroadenomas. It is unclear what strain level and strain rate were used in these measurements which makes it possible that the difference in the data can be explained because the tests may have been conducted at different strain levels. Krouskop (1998) recognized that the non-linear behavior of breast tissue requires the computation of an elastic modulus at more than one strain level. At 5% precompression strain he found that the ratio of the elastic modulus of cancerous tissue to that of fat was 5:1, while at 20% precompression strain the ratio grew to 25:1. However these previous characterizations give at most a two-point measurement of the stress-strain relationship and do not characterize it adequately for all strain levels. Any new method of documenting and diagnosing breast cancer through stiffness measurements needs a thorough characterization of the tissue for all strain levels that we present.

We also pose more fundamental questions, is there a relationship between tissue stiffness or change in the stiffness with strain level and histological diagnosis? To answer both of these questions we have made a series of measurements of the mechanical properties of a variety of breast tissues, both normal and abnormal, in compression. We have computed their elastic moduli and the constants to an exponential fit to the nominal stress – nominal strain data computed from force displacement data measured during punch indentation tests.

Methods

We have constructed a portable testing device that can be used in the operating room to measure the mechanical properties of tissue immediately after it is removed from the body because it is unknown how much they will change with time (Fung 1993). The testing instrument shown in Figure 1(a) is used for both uniaxial compression tests and punch indentation tests of tissue by replacing the punch indenter shown with a 40 mm diameter flat plate. A vacuum clamping fixture stabilizes the resected sample that has been cut to a uniform thickness and placed directly beneath the indenter as shown in Figure 1(b). The examiner applies repeated loads to the sample with a 4mm diameter flat-bottomed punch while the force applied by the punch to the sample is measured using a uniaxial load cell (Omega Miniature F1000, Omega Engineering Ltd., Stamford, CT). The load cell is amplified using an instrumentation amplifier and has a full-scale range of +/- 9.8 N. The punch position is measured simultaneously using a linear potentiometer (Midori GreenPot LP100F-5K, Midori America Corporation, Fullerton, CA), with a range of 100 millimeters. Data is acquired from each transducer at 2 kHz using a PCMCIA analog to digital card (PCMCIA16XE50, National Instruments Corp., Austin TX) and data acquisition software running on a laptop computer. After calibration, the uniaxial transducer has a measured gain of 0.994 ($r^2=1.000$) with accuracy better than 5 mN and resolution of 0.16 μ N. The potentiometer has measured gain of 1.000 ($r^2=1.000$) with accuracy better than 13 μ m and a resolution of 1.5 μ m. Given a maximum load of 4.9 N, applied over a minimum resolvable difference of 13 μ m, these noise specifications imply that the maximum resolvable elastic modulus is on the order of 40 MPa. The maximum stiffness measurable with the instrument is set by the intrinsic mechanical

stiffness of it with the 4 mm punch in place and is 28 MPa, assuming a 1mm thick sample.

In order to estimate the elastic modulus of the tissue from the punch indentation tests we will assume that the different types of tissue (tumor, normal glandular, fat etc.) can be modeled as homogeneous, and that their behavior in compression can be modeled as approximately isotropic. Further, we will make the assumption, as have other researchers (Fung 1993, Krouskop 1998), that the tissue is approximately incompressible. This implies that the Poisson ratio is 0.5, and that only an elastic modulus is required to characterize the tissue - provided we also assume that viscous effects are negligible. We will investigate the viscous effects by varying the indentation speed.

In order to determine the elastic moduli of the tissue at various strain levels we need a mathematical model that relates the nominal stress and nominal strain developed during punch indentation tests to these moduli. This model must account for the apparent increase in stiffness that is due to the geometric non-linearity introduced by the thinness of the sample. Fortunately, Hayes (1971) and Zhang (1997) present a correlation that can be adapted for this purpose. For a thin specimen of linearly elastic material, force and displacement are related by

$$F = \frac{8E}{3}axK(a/h, x/h) \quad (1)$$

provided we assume that the material is incompressible (Poisson ratio = 0.5). The radius of the indenter is a , the thickness of the specimen is h , and the displacement with respect to the initial contact point with the surface is $x=x_m-x_0$ as shown in Figure 2. The empirical factor $K(a/h, x/h)$ has the form

$$K = K_1(x/h) + K_0 \quad (2)$$

where the constants K_1 and K_0 are presented in Table 1. If we substitute nominal stress, $F/\mathbf{p}i^2$ and nominal strain, $\mathbf{e}_n=x/h$, we get

$$\mathbf{s}_n = E \frac{8h}{3\mathbf{p}i} (K_1 \mathbf{e}_n^2 + K_0 \mathbf{e}_n). \quad (3)$$

Now we recognize that for the tissue specimens nominal stress and nominal strain are nonlinearly related by the equation

$$\mathbf{s}_n = \frac{b''}{m''} (e^{m'' \mathbf{e}_n} - 1). \quad (4)$$

Equating Equation 3 and 4 yields,

$$E = \frac{3a\mathbf{p}}{8h} \frac{\frac{b''}{m''} (e^{m'' \mathbf{e}_n} - 1)}{(K_1 \mathbf{e}_n^2 + K_0 \mathbf{e}_n)}. \quad (5)$$

We recognize that it is possible to compensate for the geometric nonlinearity introduced by the thinness of the sample by defining

$$\mathbf{s}_n^* = E \cdot \mathbf{e}_n \quad (6)$$

where \mathbf{s}_n^* is calculated from the measured strain and Equation 4 and can be thought of as the true stress absent any geometric nonlinearity. We observe from the data that this new curve can be fit by an exponential¹

$$\mathbf{s}_n^* = \frac{b^*}{m^*} (e^{m^* \mathbf{e}_n} - 1) \quad (7)$$

which allows us to calculate E directly from the constants b^* and m^* . Differentiating Equation 3-13 with respect to \mathbf{e}_n (and ignoring the small variation in b^* with strain) gives

¹ After substituting, the stress-strain relationship still appears to be exponential in the actual data. If we substitute equation 11 into equation 12 and then equate this with the right hand side of equation 13, we get

$$\frac{b^*}{m^*} (e^{m^* \mathbf{e}_n} - 1) = \frac{\frac{3\mathbf{p}i}{8h(K_1 \mathbf{e}_n + K_0)} b}{m} (e^{m \mathbf{e}_n} - 1)$$

from which we see that $m^* = m$ and $b^* = \frac{3\mathbf{p}i}{8h(K_1 \mathbf{e}_n + K_0)} b$. The expression $\frac{3\mathbf{p}i}{8h(K_1 \mathbf{e}_n + K_0)}$ is very nearly a constant for the range of specimen sizes tested, so the observation that the curve is still an exponential should not be surprising.

$$E = b^* e^{m^* e_n} \quad (8)$$

because $\frac{\partial \mathbf{s}_n^*}{\partial e_n} = E$ from Equation 5.

These equations were verified by comparing the results of punch indentation testing of various silicone rubber specimens with uniaxial compression test measurements made of the same specimens as detailed in Wellman (1999). The measurements were repeatable to within 1.8% (one standard deviation). The punch indentation tests were well correlated to the uniaxial tests (in a linear fit the slope was 1.08, with y intercept through zero and $r^2=0.99$). Therefore these correlations overestimate the stiffness by at most 8%.

Methods

The tissues tested in this study were obtained during surgery after patients had signed a written informed consent document. To minimize any errors introduced from tissue aging after it is removed from the body, the fresh tissue samples were tested in the operating room within 10 minutes of excision, and the surgeon identified the gross type of the tissue (e.g. tumor, surrounding fat, gland etc.) A sample of the tissue was removed from the full specimen sent to a pathologist and the histological diagnosis was obtained (e.g. infiltrating ductal carcinoma). Each sample was resected to a minimum of 10mm by 10mm and a minimum thickness of 2 mm and then fixed onto the vacuum clamping apparatus shown in Figure 2. The samples were kept hydrated with saline solution, and were tested at room temperature (21 °C +/- 2.5 °C). We preconditioned the samples 10 times with a 2 N load, which was chosen to keep the peak strain in the cancerous tissue samples at less than 10%. The instrument is hand operated and therefore it was not possible to set the strain rate exactly. In order to estimate the viscous effects the data

were recorded at a minimum of four strain rates at approximately 50 percent/second, 200 percent/second, 1000 percent/second and 2000 percent/second. At least ten indentation trials were performed on each specimen.

Once the stress-strain data were recorded, they were analyzed and curves fit to them to determine the exponential fit constants and the elastic moduli at various levels of strain. Quality of fit was computed from variation accounted for, *VAF*, which is in turn computed from percent mean squared error,

$$MSE = \frac{\sum_{i=0}^n (s_{measured}(i) - s_{fit}(i))^2}{\sum_{i=0}^n (s_{measured}(i) - \bar{s}_{measured})^2} \quad (9)$$

and *VAF* is simply

$$VAF = 1 - MSE . \quad (10)$$

Results

Figure 3 shows that there is a wide range in behavior for the various samples of tissue tested. Carcinomas are seen to be highly nonlinear and quite stiff, while fat is nearly linear and extremely soft. In multiple indentation tests made at the same strain rate, there was less than a 3.5% difference in the parameters estimated, across all specimens tested. There was slightly more variation in the measurements when variations in strain rate were considered. Figures 4(a) and 4(b) show how the nominal stress – nominal strain curves vary with indentation strain rate for representative samples of infiltrating ductal carcinoma and fat, respectively. There is a less than 5% variation in the modulus estimated for the range of strain rates tested here for all kinds of tissue.

Tables 2 and 3 summarize the results of the testing for the various specimens. The values in Table 3 were computed from Equation 8 and are extrapolated to 15% strain

for the cancer specimens. This was done because pilot testing revealed that the cancer specimens were damaged by application of strain greater than 10% (the elastic modulus of the specimen at all strain levels permanently decreased when they were subjected to larger strains).

Discussion

One result of our testing is that breast tissues can be modeled as primarily elastic whose properties are independent of strain rate. Figure 4 makes it clear that there is less than a 5% change in the parameters estimated across strain rates ranging from 50 percent/second to 2000 percent/second. This result agrees with Krouskop's finding (1998). It is important to note that there is likely some long time scale force relaxation, but it is not of interest to the detection applications discussed above because they typically apply stimuli across much shorter time scales.

The major conclusion of this work is that there is a significant correlation between tissue histology and stiffness. As shown in Tables 4, cancerous tissue is not only much stiffer than fat and normal glandular tissue, but displays a much more non-linear increase in stiffness (going from about a 10:1 stiffness ratio to approximately a 50:1 ratio as strain is increased from 1% to 15%). These figures are reflected in the model fits presented in Tables 2 and 3, where the amount of nonlinearity is reflected in the constant of the exponential and the large increase in stiffness from 0.01 strain to 0.15 strain. For normal glandular tissue and fat the exponent of the exponential fit is approximately 10, while for the cancerous tissues it is approximately twice that. Matched pair t-tests reveal that there is a significant difference between the cancer and fat and the cancer and gland at all strain levels ($t=4.3$ typical, while $t_{significant} = 2.01$, for $n=7$).

The fat tissue displays a much closer to linear response than the other tissues measured (its stiffness only changes by a factor of 3 from 0.01 strain to 0.15 strain while cancerous tissue increases in stiffness more than 25 times). We note, as did Krouskop (1998), that diagnostic specificity may be gained by exploiting this change. For instance, if an image of the elastic modulus distribution throughout the breast was made at one strain level and then the strain level was doubled, all of the tissue compressed would see an increase in stiffness. However, the malignant tissues would see a greater increase, perhaps allowing them to be discriminated from the surrounding tissue with better resolution than currently available methods.

References

- Chenevert TL, Skovoroda AR, O'Donnell M and Emelianov SY. Elasticity Reconstructive Imaging via Simulated Echo MRI. *Magnetic Resonance Imaging*. 1997.
- Fung YC. *Biomechanics: Mechanical Properties of Living Tissues 2nd Edition*. Springer Verlag, NY. 1993.
- Garra BS, Cespedes EI, Ophir J, Spratt SR, Zurbier RA, Magnant CM and Fennan MF. Elastography of Breast Lesions: Initial Clinical Results. *Radiology* 1997; 202:79-86.
- Gentle, C.R. Mammobarography: a possible method of mass breast screening. *J. Biomed. Eng.*, Vol. 10. April 1988.
- Harris JR, Lippman ME, Morrow M and Hellman S. *Diseases of the Breast*. Lippincott-Raven. 1996.
- Hayes, WC, Keer, LM, Herrmann, G and Mockros, LF. A Mathematical Analysis for Indentation Tests of Articular Cartilage. *J. Biomechanics*, Vol. 5, pp541-551, 1972. Pergamon Press.
- Krouskop TA, Wheeler TM, Kallel F, Garra BS and Hall T. The Elastic Moduli of Breast Prostate Tissues Under Compression, *Ultrasonic Imaging*. **20**:151-159, (1998).
- Lerner RM, Parker KJ, Holen J, Gramiak R and Wang RC. Sono-elasticity: Medical Elasticity Images Derived from Ultrasound. *Acoustical Imaging*. Vol. 16. June 10-12. 1987.

- Muthupillai R, Lomas DJ, Rossman PJ, Greenleaf JF, Manduca A and Ehman RL. Magnetic Resonance Elastography by Direct Visualization of Propagating Acoustic Strain Waves. *Science*, vol. 269 p1854-1857. 29 September 1995.
- Sarvazyan, AP, Skovoroda, AR, Emelianov, SY, Fowlkes JB, Pipe, JG, Adler, RS Buxton, RB and Carson, PL. Biophysical Bases of Elasticity Imaging. *Acoustical Imaging*, Vol. 21. Ed. JP Jones. Plenum Press, New York, 1995.
- Sarvazyan AP, Skovoroda AR and Pyt'ev YP. Mechanical Introscopy – A New Modality of Medical Imaging for Detection of Breast and Prostate Cancer. *Eighth IEEE Symposium on Computer Based Medical Systems*. June , 1997.
- Skovoroda AR, Klishko AN, Gusakyan DA, Mayevskii YI, Yermilova VD, Oranskaya GA and Sarvazyan AP. Quantitative Analysis of the Mechanical Characteristics of Pathologically Changed Soft Biological Tissues. *Biophysics* 40:6. 1359-1364, 1995. Elsevier Science Ltd.
- Wellman PS. *Tactile Imaging*. Ph.D. Thesis. Harvard University. 1999.
- Zhang, M, Zheng, YP and Mak AFT. Estimating the effective Young's modulus of soft tissues from indentation tests – nonlinear finite element analysis of effects of friction and large deformation. *Med. Eng. Phys.* Vol. 19, No. 6 pp512-517, 1997.

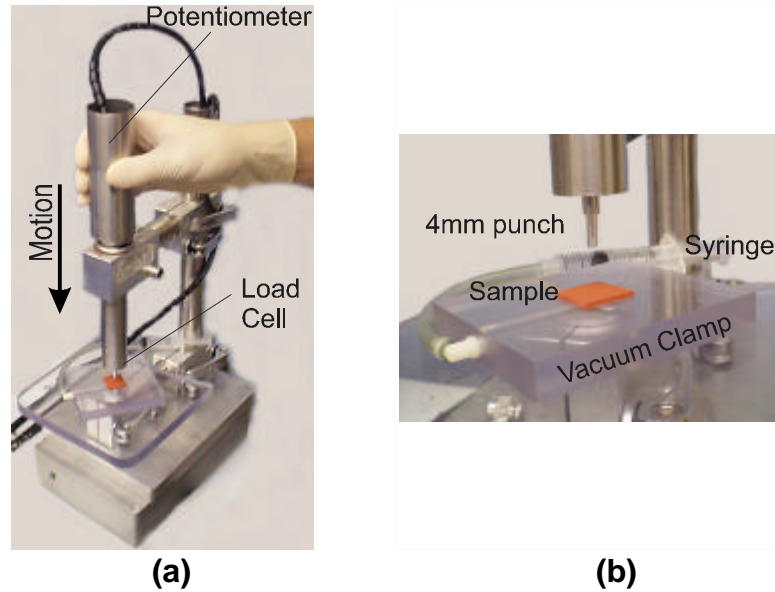


Figure 1: (a) The tissue testing instrument and a close-up photograph (b) showing the sample location and typical geometry.

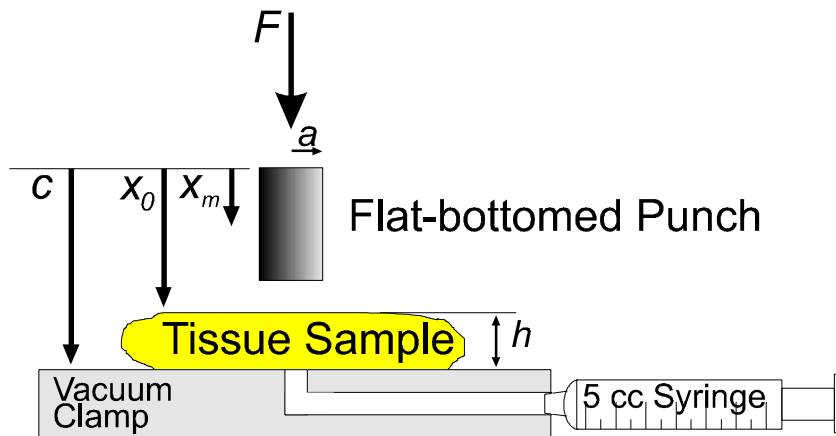


Figure 2: The specimen geometry during punch indentation testing.

a/h	$x/h = 0.01$	$x/h = 0.1$	$x/h = 0.15$	$K1$	$K0$	r^2
0.2	1.24	1.36	1.42	1.26	1.23	1.00
0.4	1.70	1.85	1.93	1.67	1.68	1.00
0.6	2.18	2.45	2.61	01	2.15	1.00
0.8	2.80	19	45	4.63	2.75	1.00
1.0	59	4.11	4.38	5.66	54	1.00
1.5	6.08	7.51	8.40	16.48	5.90	1.00
2.0	9.11	11.56	105	28.04	8.81	1.00

Table 1: Constants $K = K_1(x/h) + K_0$ for the fit to Zhang's (1997) correlation.

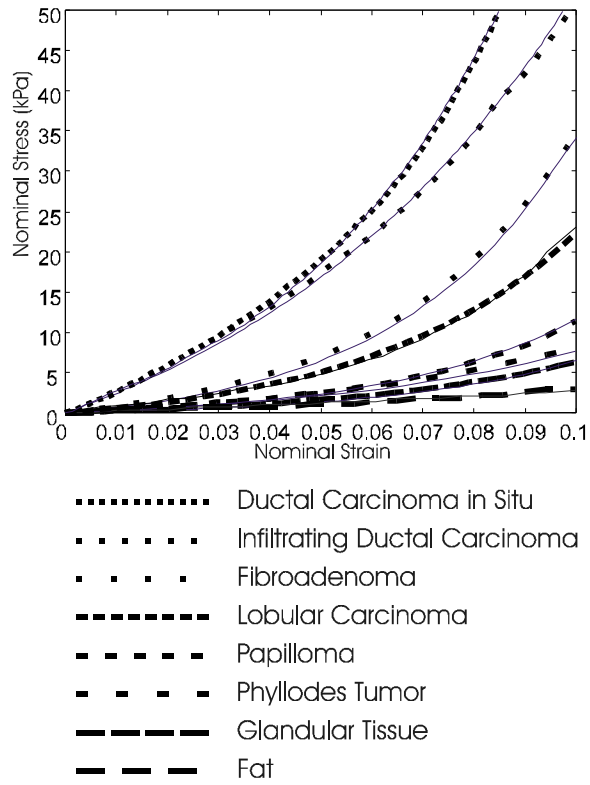


Figure 3: Typical strain-stress curves for 8 different kinds of breast tissue measured at approximately 500 percent/second indentation strain rate.

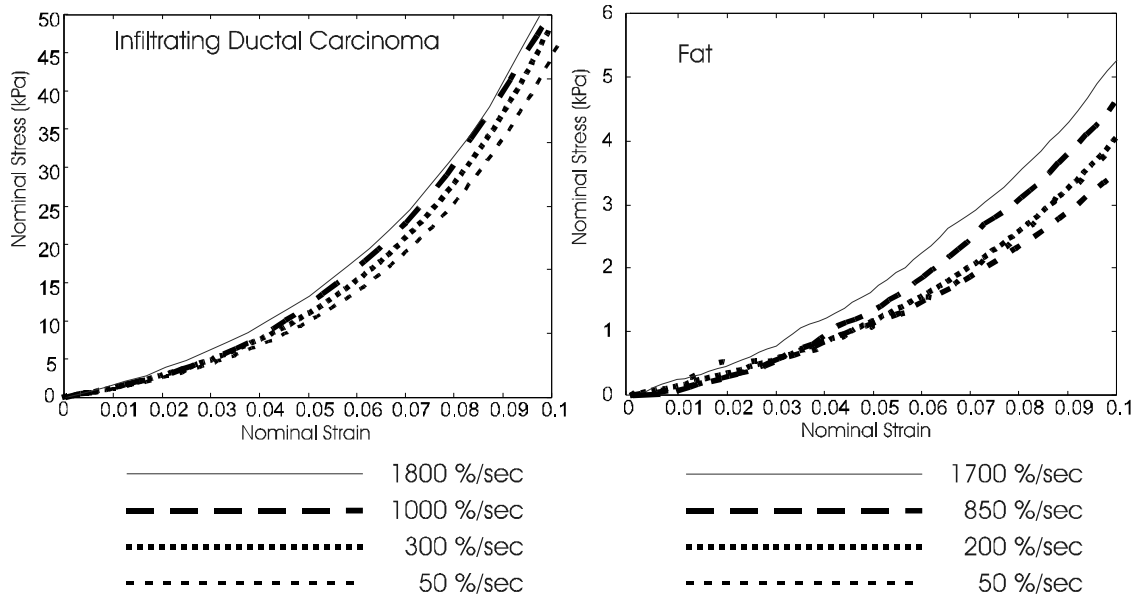


Figure 4: (a) Typical strain stress curves for infiltrating ductal carcinoma at four different velocities. There is less than a 5% difference in the modulus across all strains from the highest to the slowest indentation strain rates. (b) Typical strain-stress curves for fat at four different velocities. There is less than a 4.5% difference in the elastic modulus at all strain levels between the largest and the smallest strain rates.

Tissue Type	N	m^*	SD	b^*	SD	VAF (%)
Fat	26	7.4	4.0	4460	2345.6	98.2
Gland	7	12.3	7.4	15174.5	6750.7	96.7
Phyllodes Tumor	1	11.9	0.0	50312.8	0.0	95.9
Papilloma	2	21.4	2.8	17765.2	4201.6	98.3
Lobular Carcinoma	1	20.9	0.0	28269.6	0.0	96.5
Fibroadenoma	5	20.0	1.4	37572.4	6047.4	99.4
Infiltrating Ductal Carcinoma	25	19.9	5.5	37958.7	6146.7	97.6
Ductal Carcinoma in Situ	1	24.4	0.0	55776	0.0	97.2

Table 2: Average fit parameters for the exponential fit $\mathbf{s}_n^* = \frac{b^*}{m^*} (e^{m^* e_n} - 1)$, standard deviations of the parameters across specimens (SD), percent mean squared error (MSE) and number of samples for each of eight different types of breast tissue tested. No standard deviation is reported for those types for which there was only one specimen.

Tissue Type	Elastic Modulus at Strain 0.01	SD	Elastic Modulus at Strain 0.05	SD	Elastic Modulus at Strain 0.10	SD	Elastic Modulus at Strain 0.15	SD
Fat	4.8	2.5	6.6	7	10.4	7.9	17.4	8.4
Gland	17.5	8.6	33	12.0	88.1	66.7	271.8	167.7
Phyllodes Tumor	56.6	0.0	90.8	8.6	164.3	0.0	297.7	0.0
Papilloma	22.2	5.8	54.4	19.7	169.7	80.6	537.8	209.1
Lobular Carcinoma	34.7	0.0	78.9	0.0	221.8	0.0	628.4	0.0
Fibroadenoma	45.5	20.1	100.5	39.6	288.4	110.9	889.2	205
Infiltrating Ductal Carcinoma	47.1	19.8	115.7	42.9	384.5	126.9	1366.5	348.2
Ductal Carcinoma in Situ	71.2	0.0	188.7	0.0	638.7	0.0	2162.1	0.0

Table 3: Average elastic moduli and the standard deviation of the moduli (SD) for each of eight different types of breast tissue tested. SD is not reported for those tissue types for which there was only one specimen.

Tissue Type	Ratio to Fat at			
	Strain = 0.01	Strain = 0.05	Strain = 0.10	Strain = 0.15
Gland	4	5	8	16
Phyllodes Tumor	12	14	16	17
Papilloma	5	8	16	31
Lobular Carcinoma	7	12	21	36
Fibroadenoma	9	15	28	51
Infiltrating Ductal Carcinoma	10	18	37	79
Ductal Carcinoma in Situ	15	29	61	124

Table 4: The ratio of elastic modulus of each tissue type to fat at 4 different strain levels.